

# MULTI-OBJECTIVE DESIGN OPTIMIZATION OF AN INDUSTRIAL LDPE TUBULAR REACTOR USING JUMPING GENE ADAPTATIONS OF NSGA AND CONSTRAINT HANDLING PRINCIPLE

N. Agrawal,<sup>1</sup> G. P. Rangaiah,<sup>1\*</sup> A. K. Ray<sup>2</sup> and S. K. Gupta<sup>3</sup>

<sup>1</sup> Department of Chemical and Biomolecular Engineering, National University of Singapore, Engineering Drive 4, Singapore 117576

<sup>2</sup> Department of Chemical and Biochemical Engineering, University of Western Ontario, London, Ontario, N6A 5B9, Canada

<sup>3</sup> Department of Chemical Engineering, Indian Institute of Technology, Kanpur, 208 016, India

\* Corresponding author: Telephone: 65-6516-2187; Fax: 65-6779-1936; E-mail: [chegpr@nus.edu.sg](mailto:chegpr@nus.edu.sg)

## Abstract

Multi-objective optimization of an industrial low-density polyethylene (LDPE) tubular reactor is carried out at design stage with the following objectives: maximization of monomer conversion and minimization of normalized side products (methyl, vinyl, and vinylidene groups), both at the reactor end, with end-point constraint on number-average molecular weight ( $M_{n,f}$ ) in the product. An inequality constraint is also imposed on reactor temperature to avoid run-away condition in the tubular reactor. The binary-coded elitist non-dominated sorting genetic algorithm (NSGA-II) and its jumping gene (JG) adaptations are used to solve the optimization problem. Both the equality and inequality constraints are handled by penalty functions. Only sub-optimal solutions are obtained when the equality end-point constraint on  $M_{n,f}$  is imposed. But, correct global optimal solutions can be assembled from among the Pareto-optimal sets of several problems involving a softer constraint on  $M_{n,f}$ . A systematic approach of *constrained-dominance principle* for handling constraints is applied for the *first* time in the binary-coded NSGA-II-aJG and NSGA-II-JG, and its performance is compared to the penalty function approach.

## Introduction

Low-density polyethylene (LDPE) is one of the most widely used polymers in the world. Nearly one quarter of its annual production of 84 million tones worldwide, is produced by high-pressure technology (Kondratiev and Ivanchev, 2005). Therefore, even small improvement in polymer production and/or properties can generate large revenue for the poly-olefins industry. The end properties of polymer, viz., tensile strength, stiffness, tenacity etc. are related to molecular parameters, which include average molecular weight, polydispersity index, short- and long-chain branching, and distribution of functional groups etc. The operating and design variables often influence the molecular parameters in non-commensurable ways. Therefore, these applications are perfect scenarios for multi-objective optimization (MOO). This article presents enhancement in the production, quality and strength of LDPE, simultaneously, by MOO of an industrial high-pressure tubular reactor for ethylene polymerization at *design* stage. The non-dominated sorting genetic algorithm (NSGA-II; Deb, 2001) and its jumping gene (JG) adaptations (Simoes et al., 1999; Kasat et al., 2003; Man et al., 2004; Shrikant et al., 2006) are used to optimize the reactor performance.

Many studies on the modeling and simulation of high-pressure tubular reactor to produce LDPE have been reported in the literature, which were reviewed by Zabisky et al. (1992) and Kiparissides et al. (1993). In contrast, only some studies (Yoon and Rhee, 1985; Mavridis and Kiparissides, 1985; Brandolin et al., 1991; Kiparissides et al., 1994; Cervantes et al., 2000; Asteasuain et al., 2001; Yao et al., 2004) have appeared on the optimization of LDPE tubular reactor in the open literature. But, interestingly, all the studies on modeling used different kinetic parameters to simulate the reactor. Zabisky et al. (1992), Kalyon et al. (1994), and Brandolin et al. (1996) used

industrial data and tuned the kinetic parameters but they did not provide the complete details of either tuned kinetic rate parameters or the reactor data due to proprietary reasons. In our earlier study (Agrawal et al., 2006), we modified the model of Asteasuain et al. (2001), simulated an *industrial* high-pressure tubular reactor and tuned the model parameters using reported industrial data (Asteasuain et al., 2001). Complete details of the model including parameter values were available in Agrawal et al. (2006), and are not reported here for brevity.

Agrawal et al. (2006) used the developed model for MOO of the industrial LDPE tubular reactor at *operation* stage. The two important objectives considered for optimization were maximization of monomer conversion and minimization of normalized side products (short chain branches, vinyl, and vinylidene groups), both at the reactor exit. In this study, eleven decision variables were used to optimize the *operation* of the high-pressure tubular reactor for LDPE production. The focus of the present study is the optimization of this tubular reactor at *design* stage for multiple objectives, which involves more decision variables and hence is more challenging. As in our previous study (Agrawal et al., 2006), binary-coded NSGA-II and its JG adaptations failed to converge to the Pareto-optimal set when an hard equality constraint on  $M_{n,f}$  is imposed; however, correct global Pareto-optimal points are obtained by running several problems involving softer constraints of the type:  $M_{n,f} = M_{n,d} \pm$  an arbitrary number. These interesting results are discussed in detail.

Deb (2001) showed that the penalty parameter for handling constraints by penalty function approach plays an important role in multi-objective evolutionary algorithms. If the parameter is not chosen properly then it may create a set of infeasible solutions or a poor distribution of solutions. Thus, a systematic approach of *constrained-dominance principle* for handling constraints was proposed by Deb (2001). Motivated by these, *constrained-dominance principle* is successfully implemented in the binary-coded NSGA-II-aJG and NSGA-II-JG for handling constraints for the *first* time and its effectiveness is evaluated for design stage optimization of an industrial LDPE reactor.

## Process Description

Commercially, LDPE is produced in tubular reactors, which consist of several tubes connected together with 180° bends. This is a well-established technology for producing LDPE worldwide. The tubular reactor (Asteasuain et al., 2001; Fig. 1) used in our study, is 1390 m long and 0.05 m in diameter. The tubular reactor is divided into five zones, which are decided due to change in jacket fluid temperature and/or introduction of initiators. The monomer (ethylene), solvent (n-butane), and oxygen (an initiator) are fed into the reactor at 2250 atm and 76°C. The reaction mixture is preheated in the first two zones and then initiator,  $I_1$ , is injected in the third zone to start the polymerization reaction. The reaction mixture reaches 325–335°C due to large heat of reaction. Therefore, to avoid run-away condition, reactant–product mixture is cooled in the third and fourth zones using cooling water flowing counter-currently in the jackets. In order to further increase the monomer conversion, initiator,  $I_2$ , is fed into the fifth zone. Later part of this zone acts as a cooler to reduce the mixture temperature to ease separation in downstream operations. The monomer conversion per pass is about 30% at the reactor exit. Solvent is used to control the molecular weight of polyethylene by the process of chain transfer to the solvent. The number-average molecular weight of the polymer at the reactor exit is reported to be 21900 kg/kmol.

For simulating the industrial LDPE reactor, the dynamic model of Asteasuain et al. (2001) is modified to the steady-state model (Agrawal et al., 2006). In brief, the model is based on plug flow assumption, and incorporates axial variation of concentration, temperature, pressure and hence physical properties, and also several main (Asteasuain et al., 2001) and side reactions, e.g., intra-molecular chain transfer, chain transfer to polymer,  $\beta$ -scission of secondary and tertiary radicals etc. (the latter give the extent of long- and short-chain branching and the amount of unsaturation). Details of all the model equations, parameter values, and model validation are reported elsewhere (Agrawal et al., 2006).

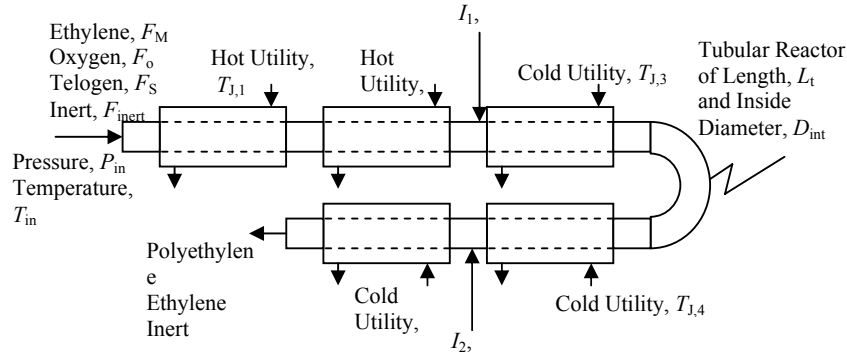


Fig. 1. Schematic diagram of an industrial LDPE reactor (Asteasuain et al., 2001).

### Multi-objective Optimization

For the design stage MOO study of the industrial tubular LDPE reactor, twenty-two decision variables are used: the inlet temperature ( $T_{in}$ ), the feed flow rates of oxygen ( $F_o$ ), solvent ( $F_s$ ) and the two additional initiators ( $F_{I,1}$ , and  $F_{I,2}$ ) added in-between, the five average jacket fluid temperatures ( $T_{J,1} - T_{J,5}$ ), the inlet pressure ( $P_{in}$ ), the axial lengths of five zones ( $L_{z1} - L_{z5}$ ), inside diameter ( $D_{int}$ ), jacket diameter ( $D_{Jacket}$ ), and flow rates of the jacket fluid ( $V_{J,2} - V_{J,5}$ ). Note that  $D_{int}$  and  $D_{Jacket}$  are constant for all zones. Saturated steam is used to preheat the reaction mixture in the first zone and therefore jacket fluid flow rate for zone one ( $V_{J,1}$ ) is not included as a decision variable. The monomer feed rate ( $F_M$ ) to the reactor is kept constant in this study. The details of the MOO problem for simultaneous maximization of conversion and minimization of normalized side products at the reactor exit are shown in Eq. 1. The variables:  $L_{z1} - L_{z5}$ ,  $D_{int}$  and  $D_{Jacket}$  are allowed to vary within  $\pm 20\%$  of their reference values (mostly industrial values). The bounds for  $V_{J,2} - V_{J,5}$  are chosen based on industrial practice (Kalyon et al., 1994). Lower limit of  $F_s$  is changed to  $5 \times 10^{-2}$  kg/s (it was  $2 \times 10^{-2}$  kg/s in operation stage optimization) because simulation was found taking an excessive CPU time for *some* chromosomes. Bounds on other decision variables are same as in our previous study (Agrawal et al., 2006).

A local constraint,  $T_{max}(z) \leq T_{max,d} (= 610.15 \text{ K})$ , is imposed on the temperature in the reactor to ensure safety, while the number average molecular weight,  $M_{n,f}$  of the product is constrained to lie (exactly) at a desired value ( $M_{n,d} = 21,900 \text{ kg/kmol}$ ). Both the equality and inequality constraints are incorporated in the objective functions in the form of penalty functions with weighting factors of  $w_1 = 10^9$  and  $w_2 = 10^{10}$ , respectively. This is not required if constraints are handled directly through the *constrained-dominance principle*. Mathematical formulation of above problem as follows:

$$\text{Max } G_1 \equiv X_{M,f} - w_1 \left( 1 - \frac{M_{n,f}}{M_{n,d}} \right)^2 - w_1 \left\langle 1 - \frac{T_{max}(z)}{T_{max,d}} \right\rangle^2 \quad (a)$$

$$\text{Max } G_2 \equiv \frac{1}{1 + \left( \frac{[M_e]_f}{30} + \frac{[V_i]_f}{0.1} + \frac{[V_{id}]_f}{0.7} \right)} - w_2 \left( 1 - \frac{M_{n,f}}{M_{n,d}} \right)^2 - w_2 \left\langle 1 - \frac{T_{max}(z)}{T_{max,d}} \right\rangle^2 \quad (b)$$

Subjected to the following bounds:

$$5 \times 10^{-5} \leq F_o \leq 10 \times 10^{-5} \text{ kg/s} \quad (c)$$

$$2 \times 10^{-2} \leq F_s \leq 0.5 \text{ kg/s} \quad (d)$$

$$5 \times 10^{-5} \leq F_{I,1} \leq 5 \times 10^{-3} \text{ kg/s} \quad (e)$$

$$5 \times 10^{-5} \leq F_{I,2} \leq 5 \times 10^{-3} \text{ kg/s} \quad (f)$$

$$413.15 \leq T_{J,m} \leq 543.15 \text{ K} ; m = 1, 4, 5 \quad (g)$$

$$473.15 \leq T_{J,n} \leq 543.15 \text{ K} ; n = 2, 3 \quad (h)$$

$182.39 \leq P_{in} \leq 248.25$ MPa	(i)
$50 \leq L_{z1} \leq 70$ m	(j)
$80 \leq L_{z2} \leq 120$ m	(k)
$140 \leq L_{z3} \leq 220$ m	(l)
$400 \leq L_{z4} \leq 600$ m	(m)
$430 \leq L_{z5} \leq 650$ m	(n)
$0.04 \leq D_{int} \leq 0.06$ m	(o)
$0.1778 \leq D_{Jacket} \leq 0.2286$ m	(p)
$0.5 \times 10^{-3} \leq V_{J,m} \leq 25 \times 10^{-3}$ m <sup>3</sup> /s ; $m = 2, 3, 4$	(q)
$0.1 \times 10^{-3} \leq V_{J,5} \leq 25 \times 10^{-3}$ m <sup>3</sup> /s	(r)

Local constraints:

Model equations (Agrawal et al., 2006) (s) (1)

Preliminary optimization results showed that the jacket fluid velocities in second and third zones were becoming quite low and consequently large temperature change in the jacket fluid. Therefore, constraints on jacket fluid velocities were added in the mathematical formulation as shown in Eq. 2. These bounds on the jacket fluid velocities are based on the typical range reported in the literature (Coulson et al., 1996).

$$0.3 \leq v_{J,m} \leq 1.0 \text{ m/s}; m = 2, \dots, 5 \quad (2)$$

## Results and Discussion

The MOO problem was solved using NSGA-II and its JG adaptations. Initially, penalty function approach was employed for handling constraints. The best values of the computational parameters in the NSGA-II algorithms for generating solutions of the design problem are provided in Table 1. These values for NSGA-II are same as those used in operation stage MOO as reported in Agrawal et al. (2006). The computer code was run on a HP workstation (3.60 GHz and 3.25GB RAM). The CPU time on this machine was nearly 8 hours for a typical optimization run for 1000 generations involving 200 chromosomes. This machine can perform 325 MFlops according to the LINPACK program (available at <http://www.netlib.org>) for a matrix of the order of 500.

**Table 1.** Values of the computational parameters used in binary-coded NSGA-II, NSGA-II-JG, and NSGA-II-aJG for two-objective design optimization problem

Parameter	Penalty function approach			Constrained-dominance principle		
	NSGA-II	NSGA-II-JG	NSGA-II-aJG	NSGA-II	NSGA-II-JG	NSGA-II-aJG
$N_{gen}^*$	3000	3300	2500	4500	3200	3000
$N_{pop}$	200	200	200	200	200	200
$l_{substr}$	30	30	30	30	30	30
$l_{chrom}$	660	660	660	660	660	660
$l_{aJG}$	---	---	70	---	---	70
$p_c$	0.95	0.9	0.8	0.95	0.9	0.8
$p_m$	0.015	0.005	0.01	0.015	0.005	0.01
$p_{JG}$	---	0.8	0.8	---	0.6	0.3
$S_f$	0.95	0.9	0.6	0.95	0.3	0.1

\* Number of generations required for convergence for the case of  $M_{n,f} = 21900 \pm 200$  kg/kmol

First, the design problem with the equality constraint on number-average molecular weight was solved using NSGA-II. It was observed that some non-dominated solutions were obtained rather than the Pareto-optimal solutions (Fig. 2), which are perhaps the local optimal solutions. NSGA-II

took a large number (10000) of generations to give the converged solutions for this case. Now, the end-point constraint on  $M_{n,f}$  was relaxed to lie within  $\pm 1\%$  (which is well within the experimental error) of the desired molecular weight ( $M_{n,d}$ ), in particular,  $M_{n,f} = 21900 \pm 200$  kg/kmol,  $M_{n,f} = 21900 \pm 20$  kg/kmol, and  $M_{n,f} = 21900 \pm 2$  kg/kmol. For the first problem of  $M_{n,f} = 21900 \pm 200$  kg/kmol, the Pareto-optimal set was obtained using NSGA-II with good distribution (spread) of points as shown in Fig. 2. Hereafter, the Pareto-optimal set obtained for  $M_{n,f} = 21900 \pm 200$  kg/kmol case is referred as the reference Pareto-optimal set.

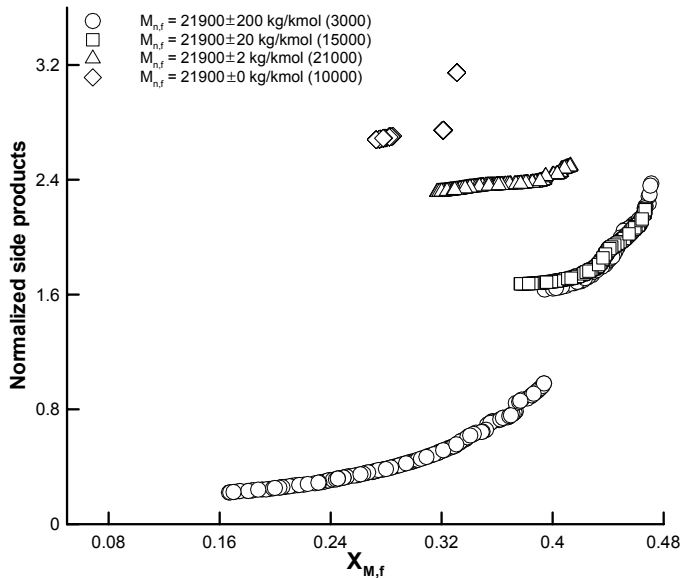


Fig. 2. Converged solutions for several end-point constraints on  $M_{n,f}$  using NSGA-II. Numbers in parenthesis refer to the number of generations.

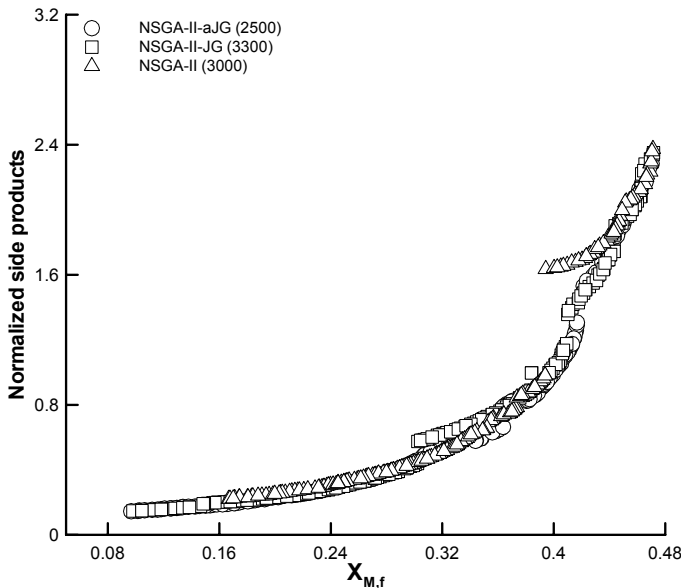


Fig. 3. Converged Pareto-optimal sets for  $M_{n,f} = 21900 \pm 200$  kg/kmol using NSGA-II and its JG adaptations.

The solutions of second problem ( $M_{n,f} = 21900 \pm 20$  kg/kmol) superimposed on the Pareto-optimal set of first problem (Fig. 2), giving confidence on the solutions obtained. However, the solutions of  $M_{n,f} = 21900 \pm 0$  kg/kmol, are quite far away from the reference Pareto-optimal set. The solutions of  $M_{n,f} = 21900 \pm 2$  kg/kmol, which has a small variability in  $M_{n,f}$ , did not converge to the

reference Pareto-optimal set, even after 21000 generations (Fig. 2). (NSGA-II-aJG and NSGA-II-JG seems to be converging to the same Pareto set in 19500 and 18000 generations, respectively; which is discussed later) This shows that NSGA-II is converging to the local or sub-optimal solutions when MOO problem includes the equality constraint on molecular weight.

In order to improve upon the optimization results, NSGA-II-aJG and NSGA-II-JG were endeavored. The best values of computational parameters in both these algorithms are also reported in Table 1, which are same as in Agrawal et al. (2006). For the  $M_{n,f} = 21900 \pm 200$  kg/kmol case, the converged Pareto-optimal sets for NSGA-II, NSGA-II-JG, and NSGA-II-aJG are shown in Fig. 3. NSGA-II-aJG produced the best Pareto-optimal set in terms of convergence and distribution of points followed by NSGA-II-JG. The converged Pareto front using NSGA-II has some non-optimal solutions, a large intermittent break, and limited diversity of solutions. In addition, NSGA-II-aJG took the least number of generations (2500) in converging to Pareto-optimal solutions in comparison to NSGA-II-JG (3300) and NSGA-II (3000).

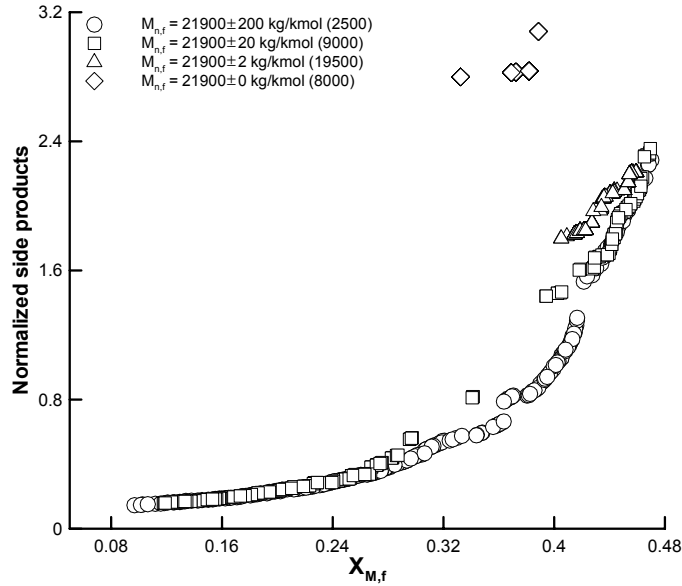


Fig. 4. Converged Pareto sets for problems having different end-point constraints on  $M_{n,f}$  using NSGA-II-aJG.

The converged Pareto-optimal sets are shown in Fig. 4 for various end-point constraints on  $M_{n,f}$  ( $\pm 200$  kg/kmol,  $\pm 20$  kg/kmol, and  $\pm 2$  kg/kmol) using NSGA-II-aJG.  $M_{n,f} = 21900 \pm 20$  kg/kmol showed slow convergence and took 9000 generations to converge to the reference Pareto-optimal set of  $M_{n,f} = 21900 \pm 200$  kg/kmol, whereas  $M_{n,f} = 21900 \pm 2$  kg/kmol required 19500 generations to nearly converge to the same. Similarly, NSGA-II-JG converged to the reference Pareto set for  $M_{n,f} = 21900 \pm 20$  kg/kmol in 14000 generations, whereas  $M_{n,f} = 21900 \pm 2$  kg/kmol took 18000 generations to nearly converge to the reference Pareto (Fig. 5). Fig. 6 shows the converged Pareto-optimal sets for the  $M_{n,f} = 21900 \pm 2$  kg/kmol case using NSGA-II and its JG variants. It is clear from the figure that Pareto-optimal sets using NSGA-II-JG and NSGA-II-aJG were closer to the reference Pareto set than that using NSGA-II for  $M_{n,f} = 21900 \pm 2$  kg/kmol case. However, neither NSGA-II, NSGA-II-JG nor NSGA-II-aJG could converge to the reference (for  $M_{n,f} = 21900 \pm 200$  kg/kmol) Pareto set for  $M_{n,f} = 21900 \pm 0$  kg/kmol case. Similar results were obtained in our earlier study on the MOO of tubular reactor at operation stage (Agrawal et al., 2006). Therefore, all these results indicate that either the solutions for equality constraint on  $M_{n,f}$  are local optimal solutions or NSGA algorithms have failed.

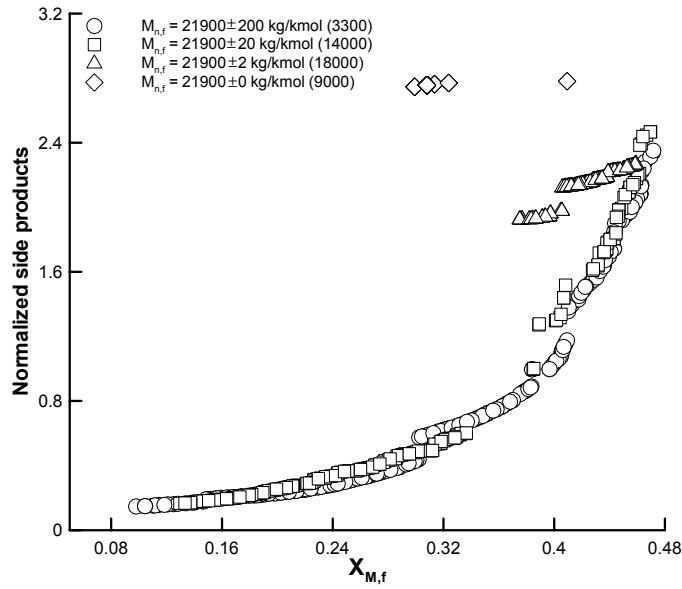


Fig. 5. Converged Pareto sets for problems having different end-point constraints on  $M_{n,f}$  using NSGA-II-JG.

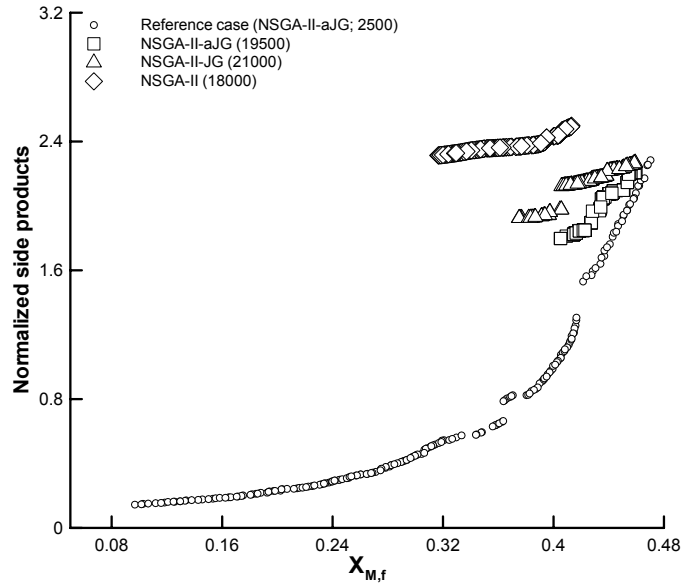


Fig. 6. Converged Pareto sets for  $M_{n,f} = 21900 \pm 2$  kg/kmol using NSGA-II and its JG adaptations. Results for NSGA-II-aJG (19500) and NSGA-II-JG (21000) are the same as those in Figs. 4 and 5, respectively.

The non-dominated solutions satisfying  $M_{n,f} = 21900 \pm 2$  kg/kmol were collected from the Pareto-optimal sets of  $M_{n,f} = 21900 \pm 200$  kg/kmol and  $M_{n,f} = 21900 \pm 20$  kg/kmol cases using NSGA-II-aJG, and are shown in Fig. 7; three (shown by open squares) and eight (shown by open triangles) solutions were collected, respectively, from these cases. These solutions were found to be covering the whole range of the reference Pareto set whereas single run of  $21900 \pm 2$  kg/kmol case distributes the non-dominated solutions in the higher conversion side (Fig. 4). High-conversion solutions are undesirable since decision maker might be interested in operating the plant at low conversion to produce higher product quality and strength (low side product concentration). Also,  $M_{n,f} = 21900 \pm 2$  kg/kmol required almost 18000 generations to converge; therefore, it involves enormous amount of CPU time. In the same CPU time, one could run four optimization cases of  $M_{n,f} = 21900 \pm 200$  kg/kmol (with different seeds or by different algorithms) or two cases of  $M_{n,f} = 21900$

$\pm 20$  kg/kmol. Therefore, we suggest to obtain *diversified* solutions near to hard equality constraints on  $M_{n,f}$  by identifying the points from among the Pareto-optimal sets of various softer constraints of type  $M_{n,f} = M_{n,d} \pm \text{arbitrary number}$ .

### Constraint Handling by Constrained-Dominance Principle

We tried to improve the performance of NSGA-II and its JG variants by incorporating *constrained-dominance principle* instead of penalty function for constraint handling. Deb (2001) showed that the penalty parameter for handling constraints plays an important role in multi-objective evolutionary algorithms. If the parameter is not chosen properly then it may create a set of infeasible solutions or a poor distribution of solutions. Therefore, the approach of *constrained-dominance principle* for handling constraints in MOO was proposed by Deb et al. (2002). Then, the *design* of an industrial LDPE tubular reactor is optimized for two-objectives using NSGA-II and its JG variants with *constrained-dominance principle* to handle the constraints. The results obtained are compared to those obtained with the penalty function method for constraint-handling in NSGA-II-aJG.

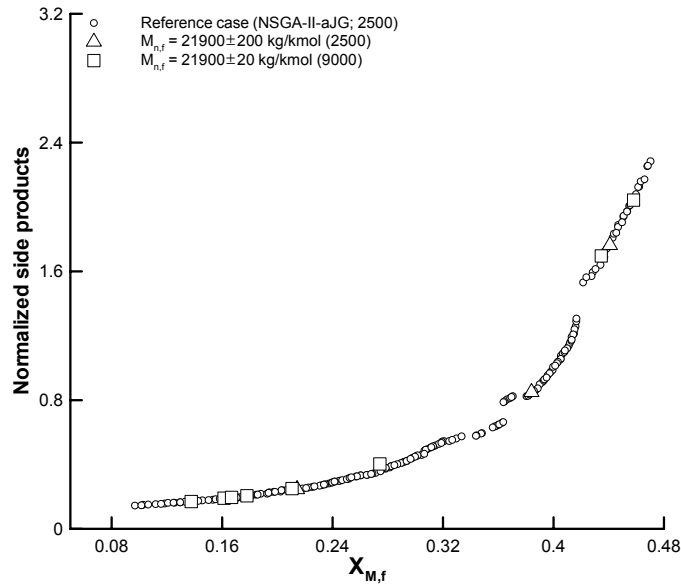


Fig. 7. Points satisfying  $M_{n,f} = 21900 \pm 2$  kg/kmol from among the Pareto sets of  $M_{n,f} = 21900 \pm 200$  kg/kmol and  $M_{n,f} = 21900 \pm 20$  kg/kmol cases using NSGA-II-aJG.

The best values of computational parameters in NSGA-II-aJG, NSGA-II, and NSGA-II-JG are obtained for *constrained-dominance principle*, and these are listed in Table 1. It was observed that the performance of NSGA-II-aJG was somewhat dependent on the random seed parameter ( $S_r$ ) and jumping gene probability ( $p_{JG}$ ) but was practically in-variant to other computational parameters. The converged Pareto-optimal set using the *constrained-dominance principle* has a slightly wider range of non-dominated points and is marginally better for the reference case ( $M_{n,f} = 21900 \pm 200$  kg/kmol) (Fig. 8); but, the *constrained-dominance principle* took more generations (3000) than the penalty function approach (2500). Note that the Pareto set using penalty function approach was not improved even after 3000 generations; these results are shown in Fig. 8 for both 2500 and 3000 generations but with a shift of 0.4 for clarity.

The Pareto-optimal set for the  $M_{n,f} = 21900 \pm 2$  kg/kmol case using the *constrained-dominance principle* is closer to the reference Pareto-optimal set than that using penalty function (Fig. 9). Similar results were obtained by the NSGA-II-JG upon inclusion of *constrained-dominance principle* for constraint handling. All these results indicate that the performances of NSGA-II-JG and NSGA-II-aJG have marginally improved when constraints are dealt with the systematic approach of *constrained-dominance principle* rather than the penalty function method. The points satisfying  $M_{n,f} = 21900 \pm 2$  kg/kmol were collected from the converged Pareto-optimal sets of  $M_{n,f} = 21900 \pm 200$

kg/kmol and  $M_{n,f} = 21900 \pm 20$  kg/kmol cases using NSGA-II and its JG variants with *constrained-dominance principle* for constraint handling. These points (Fig. 10) show uniform distribution along the reference Pareto set. This uniformity could not be captured by any algorithm along with *constrained-dominance principle* when the MOO problem with the constraint:  $M_{n,f} = 21900 \pm 2$  kg/kmol, was solved using inequality (softer) constraints with rather, non-dominated points were accumulated towards the higher end of conversion.

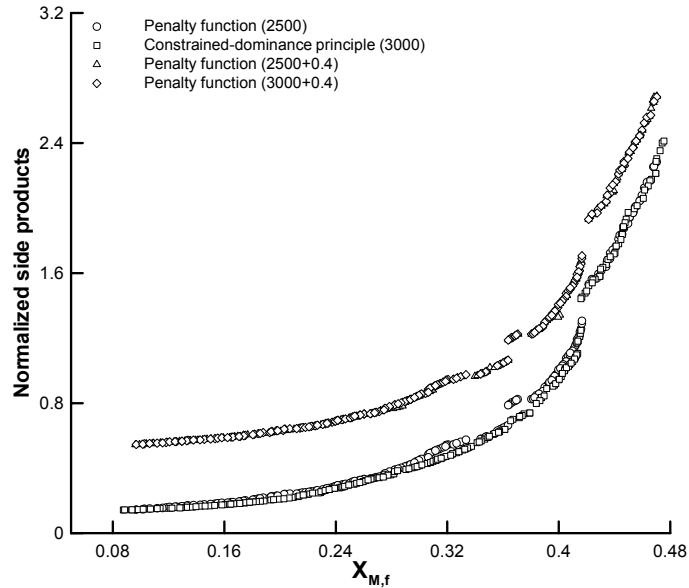


Fig. 8. Converged Pareto-optimal sets for  $M_{n,f} = 21900 \pm 200$  kg/kmol using NSGA-II-aJG for constrained-dominance principle and penalty function method. Pareto-optimal sets for 2500 and 3000 generations using the latter method are plotted with a vertical shift to show the convergence.

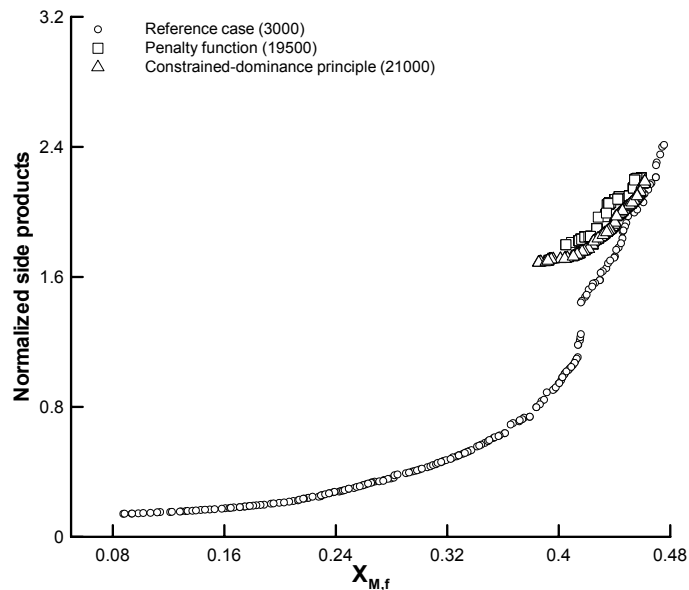


Fig. 9. Pareto-optimal solutions for  $M_{n,f} = 21900 \pm 2$  kg/kmol using NSGA-II-aJG for constrained-dominance principle and penalty function method. These solutions are compared to those for the reference case.

The Pareto-optimal set for the reference case as well as plots of the decision variables (optimal values of  $T_{in}$ ,  $T_{J,2} - T_{J,5}$  are attaining the lower extreme of the bounds whereas  $L_{Z4} - L_{Z5}$  are reaching their lower bound therefore these variables are not plotted here), and constraints

corresponding to the points in the Pareto set obtained by NSGA-II-aJG are shown in Fig. 11. When one goes from point A to point C on the Pareto-optimal set, monomer conversion increases at the expense of increased side products. The trends of decision variables:  $T_{in}$ ,  $F_o$ ,  $F_s$ ,  $F_{1,1}$ ,  $F_{1,2}$ ,  $T_{1,1} - T_{1,5}$ , and  $P_{in}$  which were used in the operation optimization of LDPE tubular reactor by Agrawal et al. (2006), are almost similar to our earlier study, and therefore effect of these variables on the Pareto set is not discussed here for the sake of brevity. Rather, the effect of appended decision variables ( $L_{z1} - L_{z5}$ ,  $D_{int}$ ,  $D_{jacket}$ , and  $V_{1,2} - V_{1,5}$ ) on the reference Pareto set of design optimization is discussed.

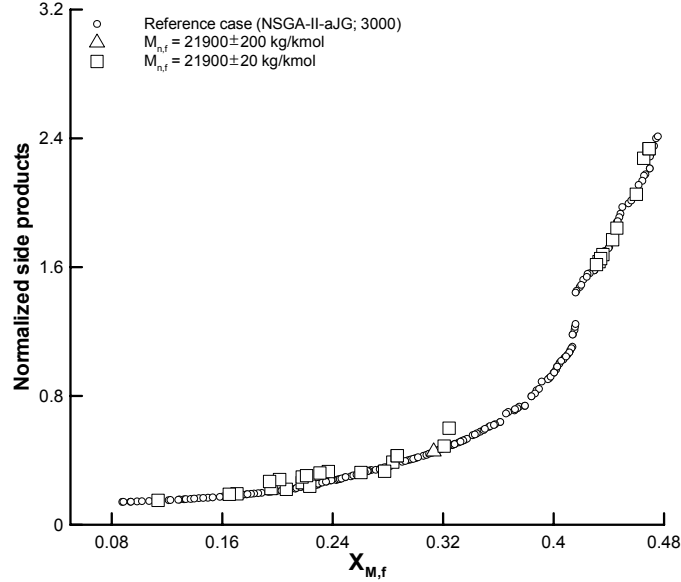
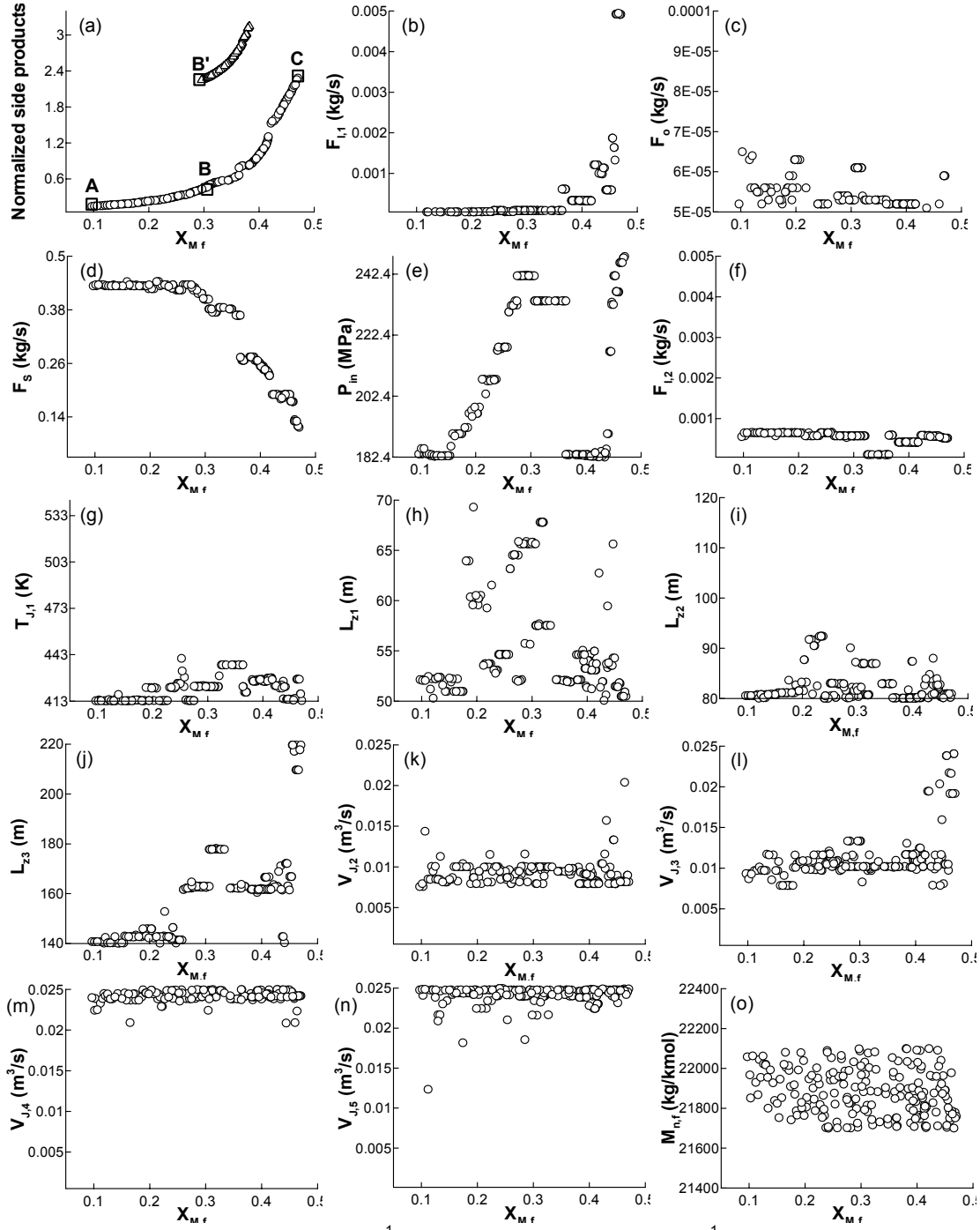


Fig.10. Points satisfying  $M_{n,f} = 21900 \pm 2$  kg/kmol from among the Pareto sets of  $M_{n,f} = 21900 \pm 200$  kg/kmol and  $M_{n,f} = 21900 \pm 20$  kg/kmol cases using NSGA-II and its JG adaptations and constrained-dominance principle.

The optimum values of  $L_{z4}$  and  $L_{z5}$  are reaching their upper bounds. The fourth zone is the cooling zone, whereas polymerization reaction takes place in the early part of fifth zone and remaining length of it is used to cool the reaction mixture. So, these two zones are cooling zones and their longer lengths keep the temperature of the reactant-product mixture low and, in turn, reduce the SCB formation. Optimal lengths of second zone ( $L_{z2}$ ) are attaining lower values to heat up the reaction mixture with higher volumetric flow rate ( $V_{1,2}$ ) in the jacket. The optimal solutions of the length of first and third zones ( $L_{z1}$  and  $L_{z3}$ ) and internal diameter ( $D_{int}$ ) are scattered. Optimal values of volumetric jacket fluid flow rates ( $V_{1,2} - V_{1,5}$ ) are attaining higher values to satisfy the constraints on jacket fluid velocities. These improve the turbulence inside the jackets and thus enhances the outside film heat transfer coefficient ( $h_o$ ) which is important for good heat transfer, and therefore the product quality. Jacket diameter ( $D_{jacket}$ ) is scattered around at its current operating value.

The solutions for design optimization are compared to the Pareto-optimal set obtained at *operation* stage optimization for the same case using NSGA-II-aJG (Fig. 11a). The results show significant improvement in the Pareto-optimal set for the design case. This improvement is attributed to the reactor temperature in design case where the maximum temperature ( $T_{max}$ ; therefore temperature inside the whole reactor) is lesser than that found in the operation stage. To illustrate this, chromosomes B and B' (identified in Fig. 11a) are selected from the Pareto-optimal sets of design and operation optimization, respectively. Monomer conversion for each of these two chromosomes is similar but normalized side products are quite different (Fig. 11a). Profiles for the temperature, monomer conversion, and initiator concentrations ( $C_{1,1}$  and  $C_{1,2}$ ) are generated for these chromosomes (along with for chromosomes A and C identified in Fig. 12a), and one shown in Fig. 12. (In Fig. 12c,  $C_{1,1}$  for chromosome A (---) is beyond the limits shown in the y-axis thus its profile could not be shown completely; rather, two vertical dashed lines are shown.) Maximum

temperature for chromosomes B and B' (Fig. 12a) is 499 K and 590 K, respectively. Therefore, the side products concentration, which decreases with temperature, is very low in design stage optimization. But, the same conversion is achieved due to gradual decomposition (unlike in the operation stage optimization) of initiators in the tubular reactor as shown in Fig. 12c. Similar trends were observed for chromosome C giving highest conversion, where temperature in the fifth zone is below the optimum temperature for decomposition of second initiator ( $I_2$ ) and then temperature of reactant-product mixture increases slowly and correspondingly monomer conversion increases (see Figs. 12a and b).



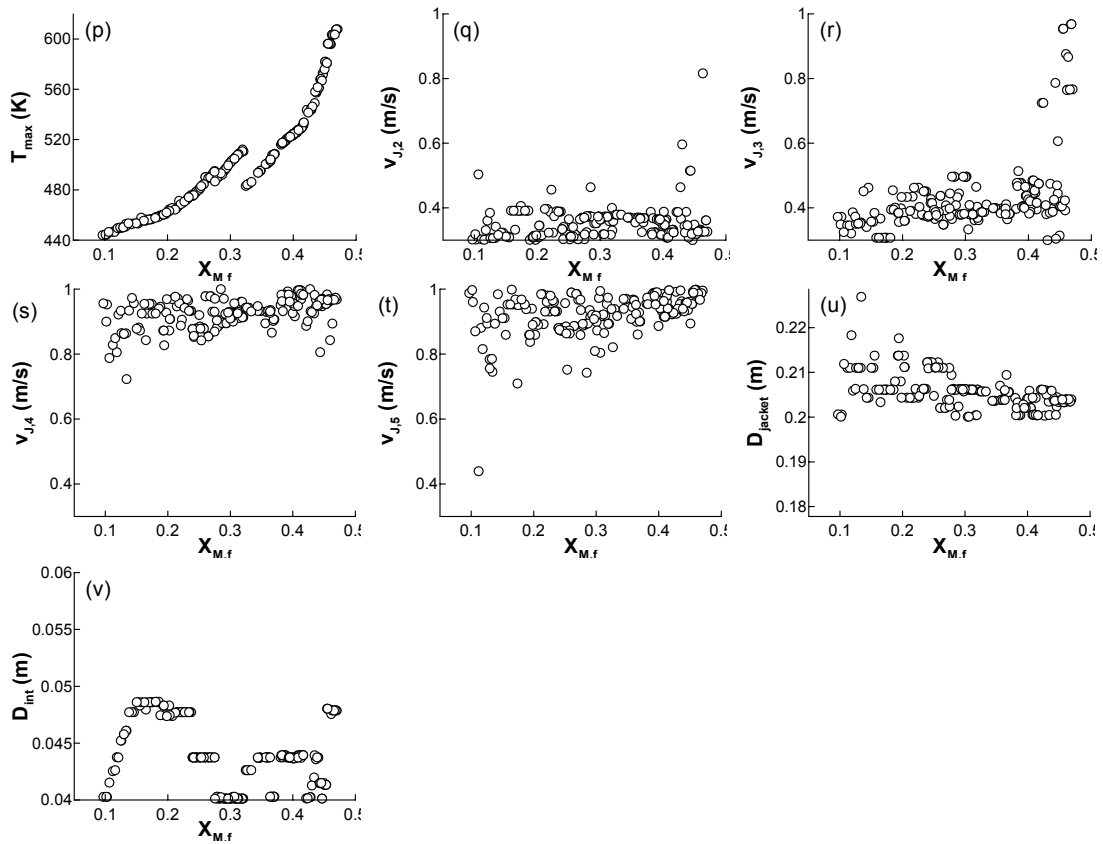


Fig. 11. Pareto-optimal points and the corresponding decision variables and constraints for the reference case ( $M_{n,f} = 21900 \pm 200$  kg/kmol) using NSGA-II-aJG.

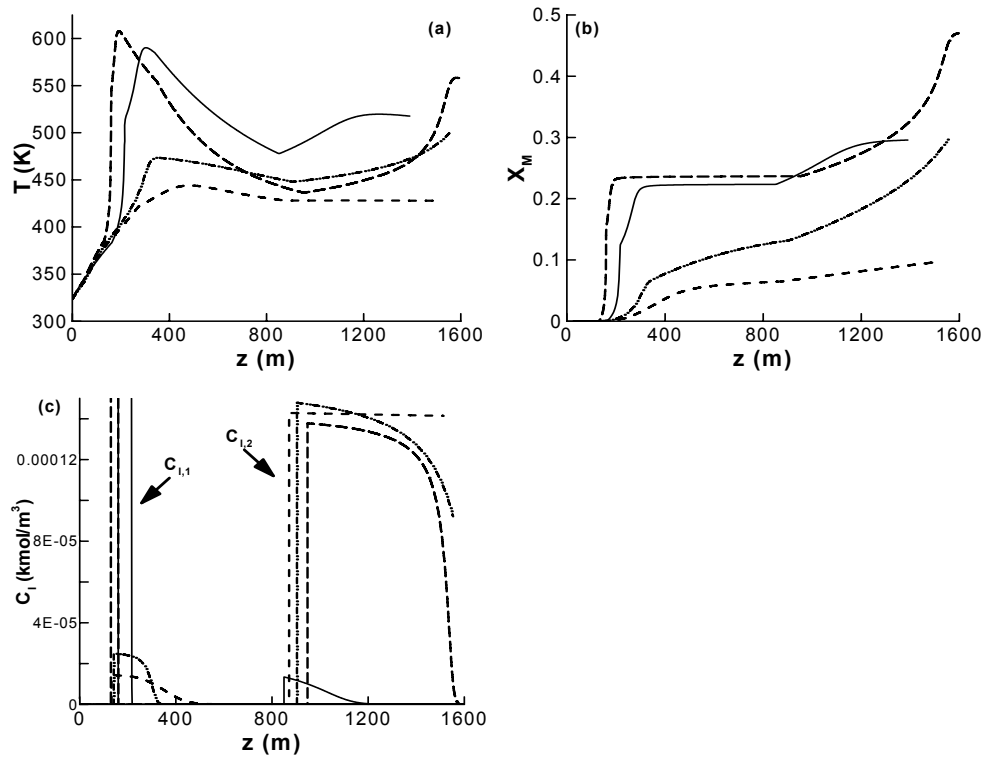


Fig. 12. Temperature ( $T$ ), monomer conversion ( $X_M$ ), and initiator concentrations profiles for chromosomes A (---), B (-·-·-), B' (—) and C (— —) shown in Fig. 11a.

## Conclusions

*Design* of an industrial tubular reactor for high-pressure polymerization of ethylene is optimized for multiple objectives using the elitist binary-coded NSGA-II and its JG adaptations. The monomer conversion is maximized and normalized side products are minimized, with constraints on  $M_{n,f}$ , reactor temperature, and jacket fluid velocities. The design stage optimization showed significant improvement in the reactor performance, when compared with the operation stage optimization. The correct global Pareto-optimal solutions could not be obtained by any of the NSGA-II, NSGA-II-JG, and NSAG-II-aJG algorithms tried, when the hard equality constraint on  $M_{n,f}$  is imposed. Comparison of the Pareto-optimal sets for  $M_{n,f} = 21900 \pm 2$  kg/kmol case obtained by the three algorithms showed that NSGA-II-aJG is better than NSGA-II and NSGA-II-JG. However, solution of this problem by any algorithm requires a lot of CPU time and the converged Pareto is limited to a small range. For the near hard end-point constraints, for instance,  $M_{n,f} = 21900 \pm 2$  kg/kmol, Pareto-optimal solutions over a wider range can be assembled from among the Pareto-optimal sets of several MOO problems with softer constraints, optimized by NSGA-II and its JG adaptations. This approach takes less CPU time too. Constrained-dominance principle worked marginally better than the penalty function approach for handling constraints in the binary-coded NSGA-II-JG and NSGA-II-aJG.

## Notation

$G_i$	$i^{\text{th}}$ objective function including penalty terms
$l_{\text{aJG}}$	length of the replacing jumping gene
$l_{\text{chrom}}$	total length (number of binaries) of a chromosome
$l_{\text{substr}}$	length (number of binaries) of a substring representing a decision variable
$L_t$	total reactor length (m)
$L_{zi}$	axial length of $i^{\text{th}}$ zone (m)
$N_{\text{gen}}$	maximum number of generations
$N_{\text{pop}}$	total number of chromosomes in the population
$p_c$	crossover probability
$p_{\text{JG}}$	jumping probability for the JG operator
$p_m$	mutation probability
$S_r$	seed for random number generator
$v_{j,i}$	velocity of coolant in the $i^{\text{th}}$ jacket (m/s)
$z$	axial distance (m)

## Subscripts

d	desired value
f	(final) reactor exit
$I,m$	$m^{\text{th}}$ initiator; $m = 1, 2$
in	inlet of reactor
J	jacket side
M	monomer
$M_e$	methyl end group
o	oxygen (initiator)
S	solvent
$V_i$	vinyl group
$V_{id}$	vinylidene group

## References

1. Agrawal, N., Rangaiah, G.P., Ray, A.K. and Gupta, S.K. (2006), "Multi-objective optimization of the operation of an industrial low-density polyethylene tubular reactor using genetic algorithm and its jumping gene adaptations," *Industrial and Engineering Chemical Research*, vol. 45, pp. 3182–3199.
2. Asteasuain, M., Tonelli, S.M., Brandolin, A. and Bandoni, J.A. (2001), "Dynamic simulation and optimization of tubular polymerization reactors in gPROMS," *Computers and Chemical Engineering* vol. 25, pp. 509–515.
3. Bhat, S.A. and Gupta, S.K. (2006), "Multi-objective optimization of an industrial semi-batch nylon-6 reactor using a new jumping gene adaptation of genetic algorithm," in preparation.
4. Brandolin, A., Lacunza, M.H., Ugrin, P.E. and Capiati, N.J. (1996), "High-pressure polymerization of ethylene. an improved mathematical model for industrial tubular reactors," *Polymer Reaction Engineering*, vol. 4, pp. 193–241.
5. Brandolin, A., Valles, E.M. and Farber, J.N. (1991), "High-pressure tubular reactors for ethylene polymerization optimization aspects," *Polymer Engineering Science*, vol. 31, pp. 381–390.
6. Cervantes, A., Tonelli, S., Brandolin, A., Bandoni, A. and Beigler, L. (2000), "Large-scale dynamic optimization of a low density polyethylene plant," *Computers and Chemical Engineering*, vol. 24, pp. 983–989.
7. Coulson, J.M., Richardson, J.F., Backhurst, J.R. and Harker, J.H. (1996), "Coulson & Richardson's Chemical Engineering: Fluid Flow, Heat Transfer and Mass Transfer," vol. I, 5<sup>th</sup> Ed., Butterworth-Heinemann: Oxford, UK.
8. Deb, K. (2001), "Multiobjective Optimization Using Evolutionary Algorithms," ed. Chichester, UK, Wiley Press.
9. Deb, K., Pratap, A., Agarwal, A. and Meyarivan, T. (2002), "A fast and elitist multiobjective genetic algorithm: NSGA-II," *IEEE Transactions on Evolutionary Computation*, vol. 6, pp. 182–197.
10. Kalyon D.M., Chiou, Y.N., Kovenklioglu, S. and Bouaffar, A. (1994), "High pressure polymerization of ethylene and rheological behavior of polyethylene product," *Polymer Engineering Science*, vol. 33, pp. 804–814.
11. Kasat, R.B. and Gupta, S.K. (2003), "Multi-objective optimization of an industrial fluidized bed catalytic cracking unit (FCCU) using genetic algorithm with the jumping genes operator," *Computers and Chemical Engineering*, vol. 27, pp. 1785–1800.
12. Kiparissides, C., Verros, G. and Pertsinidis, A. (1994), "On-line optimization of a high-pressure low-density polyethylene tubular reactor," *Chemical Engineering Science*, vol. 49, pp. 5011–5024.
13. Kiparissides, C., Verros, G. and MacGregor, J.F. (1993), "Mathematical modeling, optimization, and quality control of high pressure ethylene polymerization reactors," *Journal of Macromolecular Science-Reviews in Macromolecular Chemistry and Physics* vol. C33, pp. 437–527.
14. Kondratiev, J.N. and Ivanchev, S.S. (2005), Possibilities for optimization of technological modes for ethylene polymerization in autoclave and tubular reactors," *Chemical Engineering Journal*, vol. 107, pp. 221–226.
15. Lacunza, M.H., Ugrin, P.E., Brandolin, A. and Capiati, N.J. (1998), "Heat transfer in a high pressure tubular reactor for ethylene polymerization," *Polymer Engineering and Science*, vol. 36, pp. 992–1013.
16. Man, K.F., Chan, T.M., Tang, K.S. and Kwong, S. (2004), "Jumping genes in evolutionary computing," in *Proceedings of the Thirtieth Annual Conference of the IEEE Industrial Electronics Society (IECON)*, vol. 2, Piscataway, NJ, IEEE Press.
17. Mavridis, H. and Kiparissides, C. (1985), "Optimization of a high-pressure polyethylene tubular reactor," *Polymer Process Engineering*, vol. 3, pp. 263–290.

18. Simoes, A. and Costas, E. (1999), "Transposition: A biologically inspired mechanism to use with genetic algorithm," in *Proceedings of the Fourth International Conference on Neural Networks and Genetic Algorithms (ICANNGA99)*, Dobnikar, A. and Steele, N., Pearson, D., Portoroz, Slovenia, Springer-Verlag Press.
19. Yao, F.Z., Lohi A., Upreti, S.R. and Dhib, R. (2004), "Modeling, simulation and optimal control of ethylene polymerization in non-isothermal, high-pressure tubular reactors," *International Journal of Chemical Reactor Engineering*, vol. 2, pp. 1–25.
20. Yoon, B.J. and Rhee, H.K. (1985), "A study of the high-pressure polyethylene tubular reactor," *Chemical Engineering Communication*, vol. 24, pp. 253–256.
21. Zabisky, R.C.M., Chan, W.M., Gloor, P.E. and Hamielec, A.E. (1992), "A kinetic model for olefin polymerization in high-pressure tubular reactors: a review and update," *Polymer*, vol. 33, pp. 2243–2261.